CHEMISTRY OF MATERIALS
Article

Chem. Mater. **2009,** *21,* 4505–4514 4505
DOI:10.1021/cm9012602

General Strategy for High-Density Covalent Functionalization of Diamond Nanoparticles Using Fenton Chemistry

Roberto Martín, Patricia Concepción Heydorn, Mercedes Alvaro, and Hermenegildo Garcia*

Instituto de Tecnología Química CSIC-UPV and Departamento de Química, Universidad Politécnica de Valencia, Avenida De los Naranjos s/n, 46022 Valencia, Spain

Received May 6, 2009. Revised Manuscript Received August 12, 2009

Diamond nanoparticles (npD) from detonation do not undergo covalent functionalization to a large extent, as assessed by conventional IR and NMR spectroscopy. This low level of surface modification is due to the low density of surface hydroxyl groups and the presence of soot matter covering npD. We have found that the Fenton reaction of npD remarkably increases the density of surface OH groups, decreases the undesirable amorphous soot matter, and makes possible the subsequent high-density covalent functionalization of these nanoparticles. In this way, the polarity and solubility of npD can be controlled and, besides by IR spectroscopy, we have shown that it is even possible to characterize the resulting diamond nanoparticles by conventional solution ^{1}H NMR spectroscopy in which the signals corresponding to the proton ligands can be monitored.

Introduction

Functionalization of new allotropic forms of carbon is a topic of much current interest that could lead to a variety of smart materials with the desired properties.[1−7] In recent years, diamond nanoparticles (npD) prepared by controlled detonation have become widely available.[8,9] Considering that small nanoparticles exhibit specific properties different from those of bulk materials,[10−16] an active line of research is aimed at the chemical modification of nanoparticles by formation of covalent bond with organic moieties that can introduce new properties in the nanoparticles.[7,17−21] Compared to other allotropic forms of carbon such as fulleroids and carbon nanotubes, diamond nanoparticles constituted by sp^3 carbons are remarkable inert and devoid of chemical reactivity.[22−25] Therefore, it will be desirable to devise general strategies that could render this type of carbon nanoparticles amenable for functionalization with the required substituent density in each nanoparticle. Actually deagglomeration and covalent functionalization of npD is a topic that is presently attracting considerable attention.[26−32]

In the present work, we show that deep Fenton oxidation of npD produces a significant increase in the density of surface hydroxyl groups to the sufficient extent to introduce subsequently functional groups in npDs using conventional organic reactions. Taking into account that npD had been exploited in different fields including drug delivery, formulation of strong composites, as hard polishing materials, components in lubricant formulations

*Corresponding author. E-mail: hgarcia@qim.upv.es.

(1) Barkauskas, J. *NATO Sci. Ser., II* **2006**, *228*, 265.
(2) Hirsch, A.; Vostrowsky, O. *Funct. Org. Mater.* **2007**, 3.
(3) Rettenbacher, A. S.; Elliott, B.; Hudson, J. S.; Amirkhanian, A.; Echegoyen, L. *Chem.—Eur. J.* **2006**, *12*, 376.
(4) Rubina, Y.; Diederich, F. *Stimul. Concepts Chem.* **2000**, 163.
(5) Giordani, S.; Colomer, J. F.; Cattaruzza, F.; Alfonsi, J.; Meneghetti, M.; Prato, M.; Bonifazi, D. *Carbon* **2009**, *47*, 578.
(6) Kim, W.; Joo, J. B.; Kim, N.; Oh, S.; Kim, P.; Yi, J. *Carbon* **2009**, *47*, 1407.
(7) Krueger, A. *Chem.—Eur. J.* **2008**, *14*, 1382.
(8) Krueger, A. *Adv. Mater.* **2008**, *20*, 2445.
(9) Zhu, Z. *Mod. Phys. Lett. B* **2003**, *17*, 1477.
(10) Motornov, M.; Roiter, Y.; Tokarev, I.; Minko, S. *Handbood of Surface and Colloid Chemistry*; CRC Press: Boca Raton, FL, 2009.
(11) Areshkin, D. A.; Shenderova, O. A.; Adiga, S. P.; Brenner, D. W. *Diamond Relat. Mater.* **2004**, *13*, 1826.
(12) Sun, K. W.; Wang, J. Y.; Ko, T. Y. *J. Nanopart. Res.* **2008**, *10*, 115.
(13) Sharon, M.; Sharon, M. *Def. Sci. J.* **2008**, *58*, 460.
(14) Barnard, A. S. *Diamond Relat. Mater.* **2006**, *15*, 285.
(15) Barnard, A. S.; Russo, S. P.; Snook, I. K. *J. Comput. Theor. Nanosci.* **2005**, *2*, 180.
(16) Schatz George, C. *Proc. Natl. Acad. Sci. U.S.A.* **2007**, *104*, 6885.
(17) Yang, J.-H.; Nakano, Y.; Murakami, Y.; Song, K.-S.; Kawarada, H. *J. Nanopart. Res.* **2008**, *10*, 69.
(18) Campelj, S.; Makovec, D.; Skrlep, L.; Drofenik, M. *Mater. Tehnol.* **2008**, *42*, 179.
(19) Katz, E.; Shipway, A. N.; Willner, I. *Nanoscale Mater.* **2003**, 5.
(20) Nakamura, T.; Ishihara, M.; Ohana, T.; Koga, Y. *Chem. Commun.* **2003**, 900.
(21) Liu, Y.; Gu, Z.; Margrave, J. L.; Khabashesku, V. *Chem. Mater.* **2004**, *16*, 3924.
(22) Osawa, E. *Pure Appl. Chem.* **2008**, *80*, 1365.
(23) Kuznetsov, V. L.; Butenko, Y. V. *Ultrananocryst. Diamond* **2006**, 405.
(24) Barnard, A. S. *Ultrananocryst. Diamond* **2006**, 117.
(25) Shenderova, O. A.; Padgett, C. W.; Hu, Z.; Brenner, D. W. *J. Vac. Sci. Technol., B* **2005**, *23*, 2457.
(26) Liang, Y.; Ozawa, M.; Krueger, A. ACS Nano **2009**, ASAP.
(27) Mangeney, C.; Qin, Z.; Dahoumane, S. A.; Adenier, A.; Herbst, F.; Boudou, J.-P.; Pinson, J.; Chehimi, M. M. *Diamond Relat. Mater.* **2008**, *17*, 1881.
(28) Liu, Y.; Gu, Z.; Margrave, J. L.; Khabashesku, V. N. *Chem. Mater.* **2004**, *16*, 3924.
(29) Krueger, A.; Boedeker, T. *Diamond Relat. Mater.* **2008**, *17*, 1367.
(30) Yang, J.-H.; Nakano, Y.; Murakami, Y.; Song, K.-S.; Kawarada, H. *J. Nanopart. Res.* **2008**, *10*, 69.
(31) Krueger, A.; Liang, Y.; Jarre, G.; Stegk, J. *J. Mater. Chem.* **2006**, *16*, 2322.
(32) Lee, J.-K.; Anderson, M. W.; Gray, F. A.; John, P.; Lee, J.-Y. *Diamond Relat. Mater.* **2005**, *14*, 675.

Published on Web 09/11/2009

and microelectronics,[1,7,8,33−39] our approach can be used for the synthesis of novel materials having npD core with improved properties for these new applications.

Results and Discussion

Preliminary work carried out by us with raw npD obtained by 1,3,5-trinitrotoluene detonation shows that different reaction types as those that will be commented below fail to produce the covalent attachment of the expected groups in a sufficiently high extent to characterize the resulting materials by conventional analytical and spectroscopic techniques. We reasoned that the main causes for this failure are the low density of surface functional groups on the as-synthesized npD samples and the presence of amorphous carbonaceous material ("soot matter")[7,39] that covers the surface of crystalline npD. On the basis of this assumption, we speculated that Fenton chemistry[40−43] that produces highly aggressive $OH^{\bullet}$ radicals could serve to produce partial oxidation on the exposed surface carbons in these inert npD samples. Later, these OH groups introduced by Fenton could be used to anchor a high density of functionalities that eventually could be reflected in a substantial improvement of the ability of raw npD to undergo functionalization. In addition, the Fenton treatment could produce degradation/mineralization of the soot matter, converting it into CO_2. So far, npD functionalization has been attempted directly without prior pretreatmens.[17,44,45] Precedents of npD modification for subsequent covalent functionalization are scarce and limited to surface chlorination with Cl_2[46] and borane reduction of the carbonyl groups.[47] Our Fenton-based protocol represents a significantly improved procedure to promote high-density npD functionalization.

Fenton Treatment. Initial treatments like those usually employed in the purification of single wall carbon nanotubes consisting on ultrasonication of the npD sample in a HNO_3/H_2SO_4 3:1 solution for large periods failed to produce detectable spectroscopic changes in the npD sample.[48−52] The FT-IR spectra of the pristine npD sample and the one submitted to HNO_3/H_2SO_4 acid treatment were substantially identical. Thus, the procedure used to activate single-wall carbon nanotubes is not applicable here, revealing the higher chemical inertness of npDs compared to carbon nanotubes.

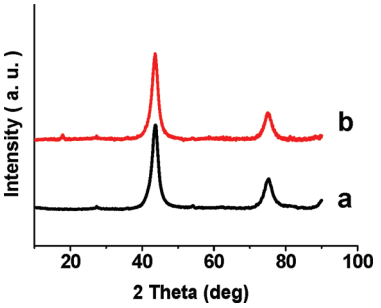

Figure 1. X-ray diffractograms of (a) pristine npD and (b) HO-npD.

Scheme 1. Fenton Reaction to Functionalize npD Surface

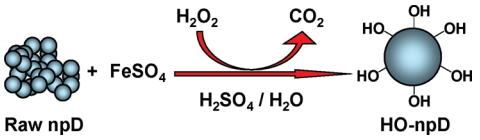

In view of these negative results and according to the previous line of reasoning, we proceeded to treat raw npD with hydrogen peroxide and a Fe(II) salt under strong acidic conditions with ultrasound irradiation. The time, ultrasound power, hydrogen peroxide concentration, and acid amount were varied to produce a chemical attack with the adequate depth to afford samples with sufficiently high density of functional groups. The harsher conditions were found to be the most convenient, and the sample resulting of the Fenton treatment under these conditions is the one denoted in the text as HO-npD (see Experimental Section). Scheme 1 illustrates the process and relevant experimental conditions.

The resulting treated sample (HO-npD) was characterized by chemical analysis, powder XRD and FT-IR and XP spectroscopies. By chemical analysis it was observed that the carbon percentage of pristine npD (95.87%) was reduced (93.28%) after deep Fenton treatment. We interpret this decrease in the carbon content (2.59%) as a reflection of the introduction of oxygen functionalities by the Fenton reaction. In XRD the typical diffraction peaks corresponding to diamond phase were maintained after the treatment indicating that HO-npD has mostly preserved the diamond crystal structure. Figure 1 shows the powder XRD of the diamond nanoparticles before and after the Fenton treatment.

(33) Holt, K. B. *Philos. Trans. R. Soc., A* **2007**, *365*, 2845.
(34) Kulisch, W. *NATO Sci. Ser., II* **2006**, *223*, 493.
(35) Faklaris, O.; Elli, A.; Joshi, V.; Sauvage, T.; Boudou, J.-P.; Roch, J.-F.; Curmi, P.; Treussart, F. Mater. Res. Soc. Symp. Proc. **2008**, *1039*, 1039.
(36) Shenderova, O. A.; Grichko, V. P. Nanodiamond UV protectant formulations. In *PCT* WO 2007027656, 2007; p 53.
(37) Chukhaeva, S. I. *Phys. Solid State* **2004**, *46*, 625.
(38) Hanada, K.; Umeda, K.; Nakayama, N.; Mayuzumi, M.; Shikata, H.; Sano, T. *New Diamond Front. Carbon Technol.* **2003**, *13*, 133.
(39) Krueger, A. *Chemistry* **2008**, *14*, 1382.
(40) Prousek, J. *Pure Appl. Chem.* **2007**, *79*, 2325.
(41) Walling, C. *Acc. Chem. Res.* **1975**, *8*, 125.
(42) von Sonntag, C. *Water Sci. Technol.* **2008**, *58*, 1015.
(43) Suty, H.; De Traversay, C.; Cost, M. *Water Sci. Technol.* **2004**, *49*, 227.
(44) Mochalin, N.; Gogotsi, Y. *J. Am. Chem. Soc.* **2009**, *131*, 4594.
(45) Spitsyn, B. V.; Gradoboev, M. N.; Galushko, T. B.; Karpukhina, T. A.; Serebryakova, N. V.; Kulakova, I. I.; Melnik, N. N. *NATO Sci. Ser., II* **2005**, *192*, 241.
(46) Spitsyn, B. V.; Davidson, J. L.; Gradoboev, M. N.; Galushko, T. B.; Serebryakova, N. V.; Karpukhina, T. A.; Kulakova, I. I.; Melnik, N. N. *Diamond Relat. Mater.* **2006**, *15*, 296.
(47) Krueger, A.; Boedeker, T. *Diamond Relat. Mater.* **2008**, *17*, 1367.
(48) Murakami, H.; Nakashima, N. *J. Nanosci. Nanotechnol.* **2006**, *6*, 16.
(49) Nakashima, N.; Fujigaya, T. *Chem. Lett.* **2007**, *36*, 692.
(50) Tasis, D.; Tagmatarchis, N.; Georgakilas, V.; Prato, M. *Chem.—Eur. J.* **2003**, *9*, 4001.
(51) Martinez, M. T.; Callejas, M. A.; Benito, A. M.; Cochet, M.; Seeger, T.; Anson, A.; Schreiber, J.; Gordon, C.; Marhic, C.; Chauvet, O.; Maser, W. K. *Nanotechnology* **2003**, *14*, 691.
(52) Alvaro, M.; Atienzar, P.; de la Cruz, P.; Delgado, J. L.; Garcia, H.; Langa, F. *Chem. Phys. Lett.* **2004**, *386*, 342.

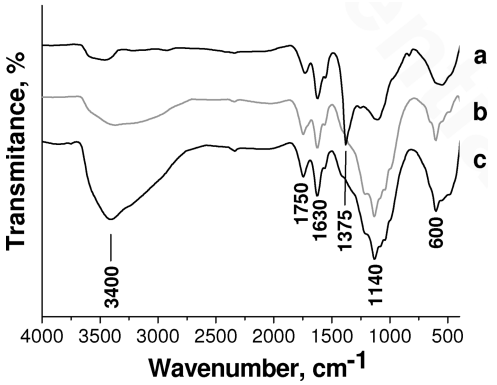

Figure 2. FT-IR spectra of (a) pristine npD, and the two samples submitted to (b) moderate and (c) deep Fenton treatment (see Experimental Section for conditions).

The types of oxygen functional groups introduced in the Fenton treatment were determined by FT-IR. Figure 2 shows a quantitative comparison of the IR spectra of npD and two HO-npD samples with medium and deep Fenton treatment. As it can be seen in this Figure, the pristine npD has a low density of isolated, not hydrogen-bonded hydroxyl groups, as well as C=O and C=C double bonds peaks at 1750 and 1630 cm^{-1}, respectively. These features are well-documented in the literature.[21,46]

Figure 2 shows that according to the conditions of the Fenton treatment the intensity of the band corresponding to hydroxyl groups, mostly hydrogen bonded, gradually grows and can became the most intense band in the FT-IR spectrum. Also it was observed a concomitant appearance of the C−O single bond at about 1200−1100 cm^{-1}. It was also noted that the C=O and C=C groups previously present in the original npD are mostly maintained during the oxidative process since the intensity of the 1750 and 1630 cm^{-1} bands remains unaltered. We propose that the C=C groups should not be exposed to the external surface and for this reason they are not altered by $OH^{\bullet}$ radical of the Fenton reaction.

X-ray photoelectron spectroscopy (XPS) provides a chemical analysis of the external surface of diamond nanoparticles. In agreement with the features observed in FT −IR spectroscopy, XPS indicates a growth of the O_{1s} peak at 533.70 eV relative to the carbon. Figure 3 shows XP spectra corresponding to untreated npD and the HO-npD sample obtained after the optimum Fenton treatment in where the growth of the O_{1s} peak corresponding to OH groups with respect to the CO by a factor of 2.2 was determined.

Thus, the previous characterization and spectroscopic data indicates that while the diamond structure is preserved (XRD), the Fenton treatment can lead to a substantial growth of the population of surface hydroxyl groups (combustion analysis, FT-IR, and XP spectroscopies). Hydroxylation of diamond nanoparticles is in full agreement with the expected outcome of Fenton chemistry considering the behavior of hydrocarbons and other aliphatic organic compounds (Scheme 1).[53,54] As commented earlier, none of the above changes were observed when pristine npD samples were treated, as is routinely performed in single-wall carbon nanotubes,[2,48,49,51,52] with mineral acid mixtures. Moreover, if single-wall carbon nanotubes are treated by Fenton under the conditions used here for npD, a complete loss of the characteristic morphology and features as determined by TEM and Raman of SWNT occurs. This indicates that SWNT cannot stand the drastic conditions of a Fenton reaction. There are in the literature also related precedents in where the morphology of single-walled carbon nanotubes is also lost when treating SWNT samples with piranha reagent that consist in a 4:1 mixture of sulphuric acid and H_2O_2.[55,56] These conditions are similar to those employed here for the deep Fenton reaction. Figure 4 shows a selected TEM image in which partial degradation of single wall carbon nanotubes can be observed after treatment under moderate Fenton conditions (see Experimental Section). Raman spectroscopy also confirms the complete degradation of single-wall carbon nanotubes after deep Fenton treatment (see Experimental Section) by the disappearance of the characteristic radial breathing mode (RBM) band specific of SWNT at about 180−250 cm^{-1} (see Figure 4).

Although out of the scope of this work these contrasting results clearly evidence the differences in reactivity and stability between SWNT and npD.

Characterization of HO-npD was also performed by transmission electron microscopy (TEM) and atomic force microscopy (AFM). Figure 4 shows selected TEM images of pristine npD and treated HO-npD samples.

Statistical analysis of the TEM images show that Fenton treatment produces a noticeable reduction in the average particle size that decreases from 7.20 nm for npD to 4.77 nm for HO-npD. Figure 5 shows the corresponding particle size distribution analysis from where the average dimensions can be determined. This size decrease can be interpreted as the result of the particle erosion with partial mineralization of the carbons to CO_2 due to the harsh Fenton treatment.

It was also noticed that the soot matter clearly visible in the TEM images of the original npD nanoparticles as a low-contrast film causing agglomeration of the nanoparticles mostly disappears after the Fenton treatment (see Figure 5). In this context, it should be mentioned that this decrease in the particle size, destruction of the soot material causing agglomeration of npD, and surface hydroxylation by Fenton should clearly be beneficial outcomes for some applications such as entrance of npD into living cells that require a control in the particle size and hydrophilicity.[57]

(53) Walling, C. *Acc. Chem. Res.* **1998**, *31*, 155.
(54) Walling, C.; Johnson, R. A. *J. Am. Chem. Soc.* **1975**, *97*, 363.
(55) Ziegler, K. J.; Gu, Z.; Shaver, J.; Chen, Z.; Flor, E. L.; Schmidt, D. J.; Chan, C.; Hauge, R. H.; Smalley, R. E. *Nanotechnology* **2005**, *16*, 539.
(56) Ziegler, K. J.; Gu, Z.; Peng, H.; Flor, E. L.; Hauge, R. H.; Smalley, R. E. *J. Am. Chem. Soc.* **2005**, *127*, 1541.
(57) Neugart, F.; Zappe, A.; Jelezko, F.; Tietz, C.; Boudou, J. P.; Krueger, A.; Wrachtrup, J. *Nano Lett.* **2007**, *7*, 3588.

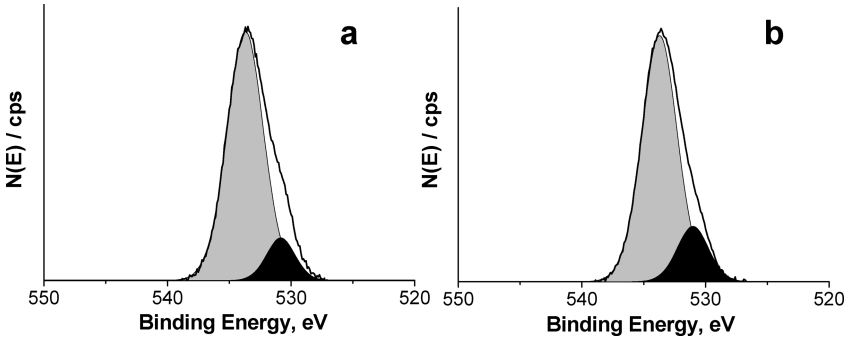

Figure 3. XPS spectra of O1s peak in (a) pristine npD and (b) HO-npD. The line corresponds to the experimental peak, whereas the black and shadowed bands are the best deconvolutions of the peak corresponding to OH and C=O, respectively.

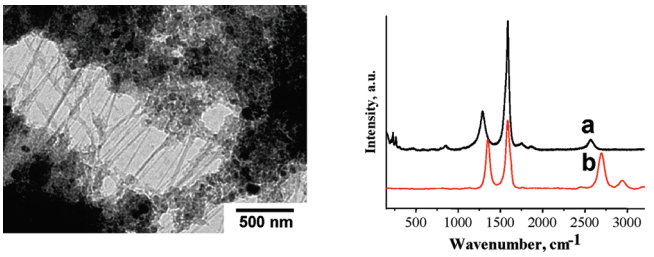

Figure 4. Left: Selected TEM image of Fenton-treated SWNT. Right: Raman spectra of (a) pristine SWNT and (b) Fenton-treated SWNT showing the disappearance of the radial breathing mode bands in the 180−250 cm^{-1} region.

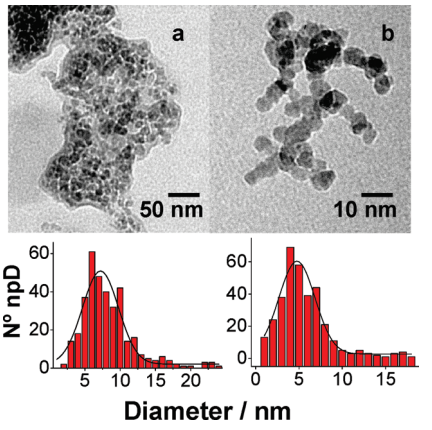

Figure 5. Selected TEM images and particle size distribution of (a) pristine npD and (b) HO-npD.

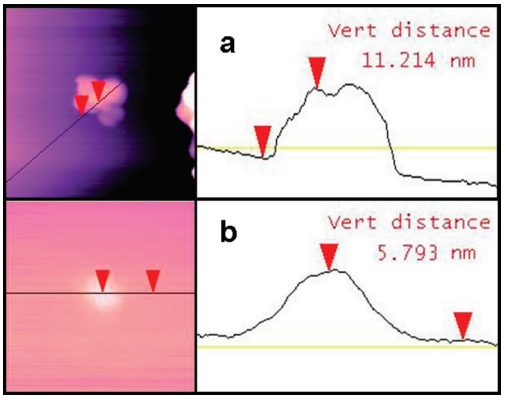

Figure 6. Selected AFM images of (a) pristine npD and (b) HO-npD after Fenton treatment.

The above conclusions drawn by TEM can also be confirmed by AFM. Figure 6 shows two AFM images of the raw npD and HO-npD. In this case the subnanometric vertical resolution of our system allows also establishing the decrease in the particle size.

Functionalization of HO-npD with Alkyl Groups. After having shown the possibility to activate npD by Fenton chemistry increasing the density of hydroxyl groups, our aim was to show that this Fenton pretreatment should exert a beneficial influence in the subsequent functionalization by other functional groups.

One of the major problems of pristine npD is the poor persistence of suspensions of these nanoparticles in organic solvents. Among other consequences, this lack of stability of npD colloidal suspensions is unfavorable to perform reactions with npD. One straightforward possibility to alleviate this inconvenient of poor "solubility" will be the anchoring of a sufficiently high density of alkyl chains on the surface of npD. These aliphatic chains should increase the affinity of the functionalized npD for organic media and eventually could serve to stabilize colloidal dispersions of npD.

On the other hand, the formation of colloidal suspensions of functionalized diamond nanoparticles in organic solvents will constitute a straightforward proof that the functionalization density achieved after the Fenton treatment is sufficiently high to dramatically change the properties inherent to npD.

A simple strategy would consist of attaching carboxylate groups to the OH functions of the HO-npD. This functionalization with alkyl chains through carboxylic esters has been previously reported in the literature to increase the compatibility of npD in organic solvents such as THF.[44,47] By borane reduction of surface carbonyl groups, a density about 0.3−0.4 mmol g^{-1} of alkyl chains has been achieved.[47] Following with this strategy, Scheme 2 illustrates the route to synthesize hydrophobic diamond nanoparticles based on the covalent attachment of alkyl chains through ester linkages.

To study the influence of the alkyl chain on the persistency of colloidal dispersions of npD in common organic solvents, we prepared five different hydrophobic C_n-npDs in which alkyl chains varied from 2 to 16 carbons. The samples were characterized by quantitative

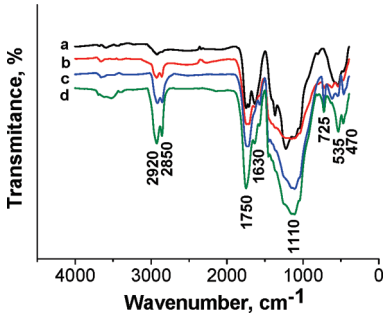

Figure 7. FT-IR spectra of identical weights (10 mg) of ester functionalized diamond nanoparticles: (a) C_1-npD, (b) C_7-npD, (c) C_{11}-npD, and (d) C_{15}-npD.

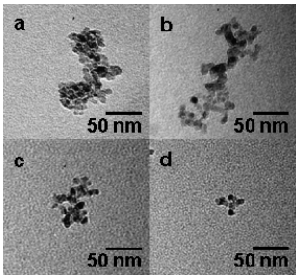

Figure 8. TEM images of alkyl-functionalized C_n-npD: (a) C_1-npD, (b) C_7-npD, (c) C_{11}-npD, and (d) C_{15}-npD.

FT-IR spectroscopy. The increasing proportion of CH_2 groups as the alkyl chain length increases was clearly observed by the intensity growth of the CH_2 stretching peaks appearing at about 2920 cm^{-1}. Figure 7 shows FT-IR spectra of identical C_n-npD weights. As can be seen there, the relative variation of two characteristic CH_2 bands increases as the length of the alkyl chain. Also, we notice that the residual population of unreacted OH groups appearing at 3600 cm^{-1} grows with the length of the alkyl chain suggesting that steric encumbrance impedes the complete reaction of the total population of OH groups when the chain length increases. In other words, the percentage of reacted OH groups is larger when the HO-npD sample is exposed to CH_3COCl and there is some residual population of unreacted OH groups for CH_3-$(CH_2)_{14}COCl$.

Selected TEM images of the alkyl functionalized C_n-npDs are shown in Figure 8. These images, corresponding to hydrophobic C_n-npDs, present many similarities in the particle size but important differences in the diminished tendency to agglomerate as compared to npD and even HO-npD. This reduced tendency to agglomerate appears to be a consequence of the increase of the chain length.

The loading of alkyl groups was determined from the comparison of the TG profiles (see Figure S1 in the Supporting Information) of the C_n-npD samples with that of the original npD. In particular, the weight loss from 150 to 500 °C, before the massive combustion of npD, was considered as due to the loss of ester groups. The results are contained in Table 1. As it can be seen there, the ester loading varies from 0.78 to 2.0 mmol g^{-1} that is between two and six times higher than the maximum loading reported using the borane procedure.[47]

As expected on the basis of the affinity of alkyl chains for organic solvents, C_n-npDs modified with carboxylate chains exhibited, as the most remarkable property, a high tendency to form indefinitely persistent colloidal suspensions in organic solvents such as CH_2Cl_2. Thus, the precursor HO-npD is a hydrophilic sample that prefers water to CH_2Cl_2. In contrast, upon esterification of the OH groups, the resulting C_n-npD prefers CH_2Cl_2 to water. The changes in the relative hydrophilicity/hydrophobicity of the samples are clearly illustrated in Figure 9 and in a video clip included in the Supporting Information. Raw npD samples sediment immediately under the same conditions.

Moreover, we notice that the sample weight that can be suspended in CH_2Cl_2 without visible settling down of any particle after 1 week increases along the number of carbons of the ester groups. Table 1 also gives the weight of sample that can form persistent suspensions in CH_2Cl_2 for each of the modified diamond nanoparticles.

Bromination of HO-npD. A reaction that has been carried out in other allotropic forms of carbon including fullerenes, graphite, and carbon nanotubes is halogenation.[2] The importance of halogenation resides in that the resulting organic halide can be a useful intermediate for further C−C functionalization.[58] Concerning npDs, fluorination and chlorination have already been reported using the corresponding halogen gases as reagents.[45,46] Herein, we have considered the use of *N*-bromosuccinimide (NBS) in CCl_4 as an experimentally convenient procedure for bromination under mild conditions (Scheme 3). We expected that Fenton treatment would also favor the reactivity of diamond nanoparticles toward bromination by removal of the soot matter and by surface hydroxylation. NBS can act as a source of Br_2 as well as HBr, provided that hydrogen atom donors are present in the medium.[14]

As expected, treatment of HO-npD with NBS produces bromination of the diamond nanoparticles. The success and the extent of the reaction were determined by chemical and XPS analyses. In combustion chemical analysis, the percentage of carbon in Br-npD respect to the HO-npD was reduced from 93.28 to 89.75%, this fact being compatible with the presence of 3.53% bromine. This percentage of bromine corresponds to 0.44 mmol g^{-1}, which is remarkable considering that we are dealing with surface functionalization and corresponds at least to one bromine atom per 170 carbon atoms. More informative are the data from XPS. Figure 10 shows the XPS measured for the Br-npD sample.

As can be seen in Figure 10, for Br-npD, a peak due to bromine atoms was clearly observed at about 70 eV. A closer look at the XPS Br_{3d} peaks shows that they are split into two components corresponding to the $Br_{3d}{}^{5/2}$ and $Br_{3d}{}^{3/2}$ contributions. Moreover, for the Br-npD sample, we noticed that the C_{1s} peak exhibits two components

(58) Gomez-Escalonilla, M. J.; Atienzar, P.; Fierro, J. L. G.; Garcia, H.; Langa, F. *J. Mater. Chem.* **2008**, *18*, 1592.

Scheme 2. Route Followed for the Synthesis of Organophilic C_n-npD

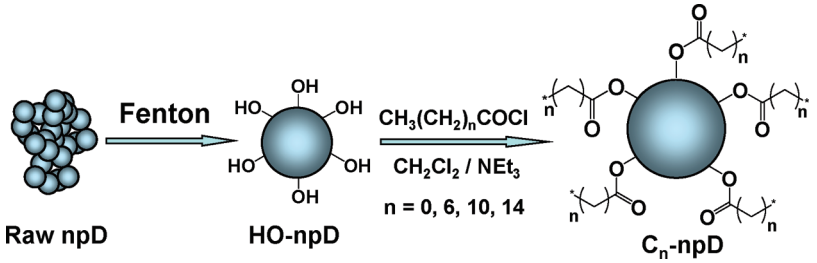

Table 1. Loading and solubility in CH_2Cl_2 of alkyl functionalized Cn −npD

sample	HO-npD	C_1-npD	C_7-npD	C_{11}-npD	C_{15}-npD
loading of alkyl chains (mmol C_n/g)[a]	0	2.0	0.79	0.82	0.78
residual population of free OH (%)[b]	100	< 1	< 1	2	6
solubility (mg of C_n-npD/mL)	0	1	4	7	16

[a] A density of 0.3−0.4 mmol (g of carboxylate groups)$^{-1}$ (from C_5 to C_{17}) has been reported for the activation of npDs by borane.[47] [b] Determined by the relative reduction of the OH vibration band in quantitative IR spectroscopy.

that can be attributed to those carbons that are bonded or not to bromine.

In sharp contrast, a control using npD not submitted to Fenton treatment did not exhibit incorporation of bromine into the diamond nanoparticles in a significant extent (detection limit 15 μmol g^{-1}) by NBS treatment as determined by combustion chemical analysis and XP spectroscopy.

Arylation of HO-npD (Martin−Garcia Reaction). One of the most typical reactions for alcohols and hydroxylic compounds is the aromatic alkylation under strong acid conditions.[59] Considering that the Fenton treatment increases the density of surface OH groups in diamond nanoparticles and considering the chemical stability of npDs, we expected that HO-npD samples should undergo arylation by electron-rich aromatic compounds under strong acid conditions.

Preliminary controls using pristine npDs suspended in anisole in the presence of anhydrous $AlCl_3$ as catalyst did not show any change after the reaction. Actually, FT-IR spectra of an npD sample recovered after the attempted arylation with anisole was coincident with that of the initial sample showing that the reaction has failed to afford arylation in a detectable extent (Figure 11). We attribute the failure of the reaction to a combination of the unfavorable influence of the presence of soot matter causing agglomeration of the nanoparticles and covering the surface of npDs as well as the low population of reactive surface hydroxyl groups.

In contrast to the behavior of original npD, the HO-npD samples readily undergo arylation under conventional Friedel−Crafts conditions. Thus, after the workup and washings of the reaction mixture, comparison of the FT-IR spectra before and after the reaction with anisole

(59) *Friedel-Crafts and Related Reactions*; Olah, G., Ed.; John Wiley & Sons: New York, 1974.

Scheme 3. Route Followed in the Synthesis of Br-npD

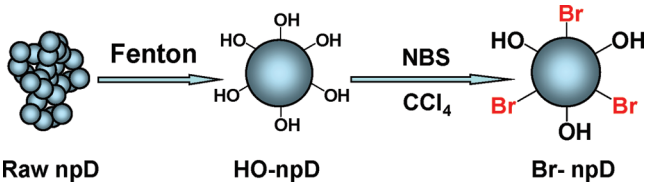

in the presence of $AlCl_3$ exhibits remarkable differences, all of them compatible with the disappearance of surface hydroxyl groups and the functionalization by 4-methoxyphenyl groups. Estimation of the percentage of anisole functionalization by thermogravimetric analysis considering the weight loss from 150 to 500 °C indicates that the loading of anisyl moieties is as high as 1.2 mmol g^{-1}. Scheme 4 illustrates the arylation reaction and Figure 11 presents representative FT-IR spectra to show the spectroscopic changes observed after the reaction.

The most reasonable mechanism to rationalize the success of the Friedel−Craft arylation of HO-npD is the nucleophilic substitution of surface hydroxyl groups by chloride under strong acid conditions that could lead to carbocation-like species formed by protonation of hydroxyl group and water elimination. These intermediates with cationic character will be intercepted by chloride from $AlCl_3$ or by the electron rich aromatic compound. Subsequently also the chloride intermediates will be eventually transformed into the final arylated derivative.

Similarly to anisole we have also undertaken the covalent functionalization of HO-npD by *N*,*N*-dimethylaniline using $AlCl_3$ as catalyst. As expected in view of the behavior with anisole, for *N*,*N*-dimethylaniline we also observed that pristine npDs were unreactive, while HO-npD readily gave the corresponding derivative (0.8 mmol g^{-1}). This was confirmed by FT-IR spectroscopy, monitoring the decrease in the population in the OH groups and the presence of the aromatic vibrations characteristics of the dimethylamino phenyl groups.

As commented in the previous section, colloidal suspensions improved in persistency when the functional groups covalently attached to the diamond nanoparticles core increase the affinity for a given solvent. Considering this, we expected that also aryl functionalized npD could be suspended in deuterated organic solvents and this could allow recording ^{1}H NMR spectra of the suspensions with sufficient resolution to have meaningful information. Our expectancies were fulfilled and ^{1}H NMR spectrum of the $MeOC_6H_4$-npD could be recorded showing

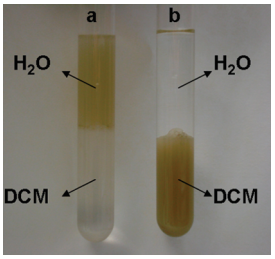

Figure 9. Different partition coefficient of nonfunctionalized and functionalized diamond nanoparticles (a) HO-npD and (b) C_7-npD in H_2O/CH_2Cl_2.

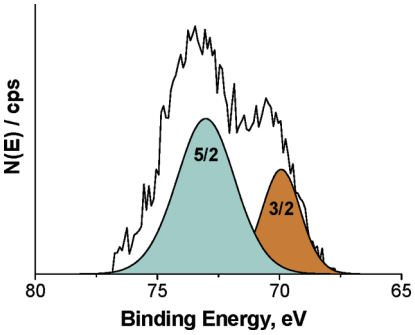

Figure 10. XPS analysis obtained for the Br-npD sample: $Br_{3d}{}^{5/2}$ peaks and $Br_{3d}{}^{3/2}$ split signals.

two doublets of the same integral corresponding to aromatic protons appearing from 7.6 to 7.2 ppm and a singlet for the three methoxyl protons observed 3.8 ppm. These features indicate substitution of one anisole aromatic hydrogen by the diamond core that behaves as a moderate electron withdrawing substituent shifting downfield the chemical shift of the aromatic hydrogens. Figure 12 shows the aromatic region of the $MeOC_6H_4$-npD ^1H NMR spectrum. Recording of solution ^1H NMR spectrum of a npD material is a remarkable achievement derived from the benefits of Fenton functionalization and it can open the way for a deeper and convincing characterization of these nanoparticles.

Functionalization of HO-npD with Heterocyclic Rings. Previously, functionalization of pristine detonation npD samples has been reported by covalent attachment through trimethoxysilyl groups.[60] Anchoring of silyl moieties to surface OH groups is a well-established methodology to functionalize materials containing surface hydroxyl groups[61] and nanoparticles including npD.[8] Herein, considering that HO-npD is a more appropriate sample for functionalization than pristine detonation npD materials, we addressed the possibility to functionalize HO-npD with viologen units using trialkoxysilyl linkers. Although in the previous section HO-npD functionalization has been carried out by Friedel–Crafts that had not been previously used to attach aromatic moieties to npD, the existing precedents about carbon nanomaterial functionalization have made ample use of the condensation reaction of trialkoxysilanes with

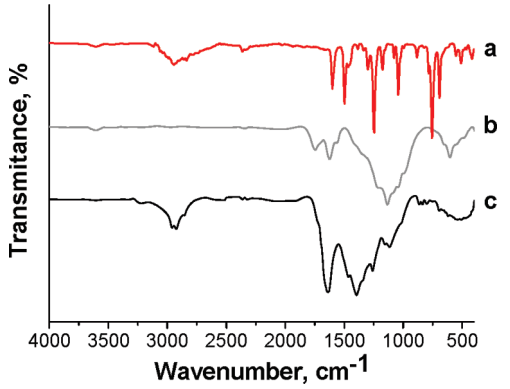

Figure 11. FT-IR spectra of (a) anisole, (b) control reaction with pristine npD, and (c) $MeOC_6H_4$-npD obtained by reaction of HO-npD with anisole.

Scheme 4. Synthetic Route Followed for the Arylation of npD with Aromatic Compounds

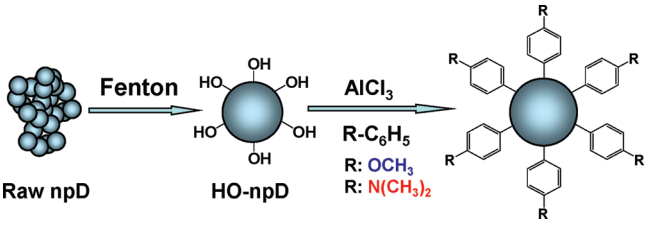

surface hydroxyl groups.[8,62] In the case considered here, the main interest of using trialkoxysilyl groups to anchor organic units is to show the contrasting behavior of npD and HO-npD after Fenton treatment even for the silylation reaction. To show this, while producing an interesting npD derivative, we selected a bipyiridinium moiety conveniently functionalized with a terminal triethoxysilyl group. Viologens exhibit many properties that can serve to implement some interesting functional response in otherwise inert diamond nanoparticles.[63–65] These properties include photo-, electro-, and thermochromism, the ability to form charge transfer complexes with electron donor species and the capability to accept electrons due to the high reduction potential of viologens.[63,66–68] The required bipyridinium derivative was prepared in two steps from 4,4′-bipyridine by methylation with iodomethane under mild conditions, followed by alkylation of 1-methyl-4-(4′-pyridyl)pyridinium iodide with (3-chloropropyl)trimethoxysilane. Finally, the compound was submitted to ion exchange to obtain the Cl^- salt. Scheme 5 shows the synthetic route followed to prepare the trimethoxysilyl viologen that was used in the functionalization of HO-npD.[69]

(60) Krueger, A.; Ozawa, M.; Jarre, G.; Liang, Y.; Stegk, J.; Lu, L. *Phys. Status Solidi A* **2007**, *204*, 2881.
(61) Corma, A.; Garcia, H. *Adv. Synth. Catal.* **2006**, *348*, 1391.
(62) Vinogradova, L. V.; Melenevskaya, E. Y.; Kever, E. E.; Zgonnik, V. N. *Vysokomol. Soedin., Ser. A Ser. B* **2000**, *42*, 221.
(63) Monk, J. A. *The Viologens: Physicochemical Properties, Synthesis and Applications of the Salts of 4,4A-Bipyridine*; Wiley: New York, 1998.
(64) Yoon, K. B.; Kochi, J. K. *J. Am. Chem. Soc.* **1989**, *111*, 1128.
(65) Komers, K. *J. Chem. Res. (S)* **1994**, 293.
(66) Dutta, P. K.; Incavo, J. A. *J. Phys. Chem.* **1987**, *91*, 4443.
(67) Dutta, P. K.; Turbeville, W. *J. Phys. Chem.* **1992**, *96*, 9410.
(68) Garcia, H.; Roth, H. D. *Chem. Rev.* **2002**, *102*, 3947.
(69) Alvaro, M.; Ferrer, B.; Fornes, V.; Garcia, H. *Chem. Commun.* **2001**, 2546.

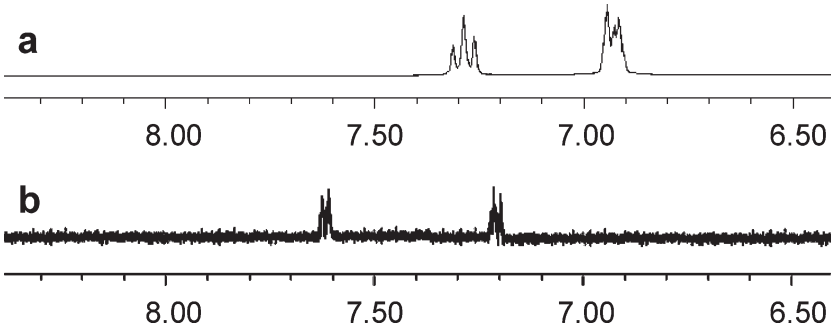

Figure 12. Expansion of the aromatic protons region of the ^{1}H NMR spectra of (a) anisole and (b) $MeOC_6H_4$-npD recorded in [d_6]-DMSO.

Scheme 5. Synthetic Route Followed to Prepare V-npD as Cl^- Salt

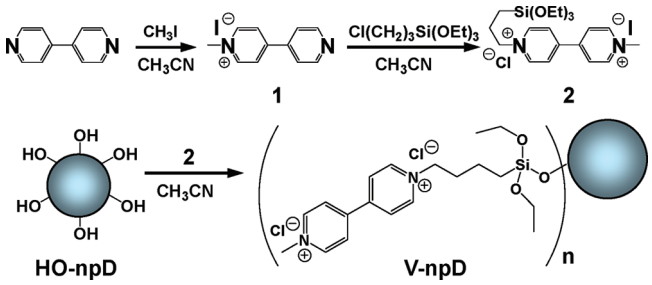

As expected in view of the different behavior between npD and HO-npD previously commented, when a suspension of diamond nanoparticles in toluene was contacted with *N*-methyl-*N*′(trimethoxysilylpropyl)-4,4′bipyridinium, characterization of the resulting nanoparticles showed that the sample of HO-npD has undergone functionalization in a significant larger extent than the pristine npD. The resulting sample was characterized by chemical and XPS analyses as well as optical and FT-IR spectroscopies. Combustion chemical analysis shows a decrease in the percentage of carbon from 93.28 to 71.58% from HO-npD to V-npD and the presence of nitrogen 5.01% in V-npD. These analytical data are compatible with the incorporation of trimethoxysilyl viologen according to Scheme 5.

XPS analysis showed also the presence of nitrogen and silicon atoms, based on their characteristic N_{1s} and Si_{2p} peaks appearing at 403.17 and 104.04 eV. Figure 13 presents the XPS data of the sample V-npD.

Quantification of the relative N/Si proportion shows the expected 2-to-1 atomic ratio for the viologen moiety, while the relative Si/C and N/C atomic ratios were 0.009 and 0.019, respectively, in agreement with the chemical analysis of the bulk sample. This analytical data correspond to a viologen loading of 1.79 mmol g^{-1} for V-npD. This high loading compares favorably with the loadings achieved for the same treatment starting with pristine npD. The data obtained by us using trialkoxysylil functionalization is not far from those previously reported for the same type of npD functionalization in previous cases.[60]

The presence of viologen units can be clearly revealed by optical and FT-IR spectroscopies. Figures 14 and 15 show the corresponding spectra characterized by an

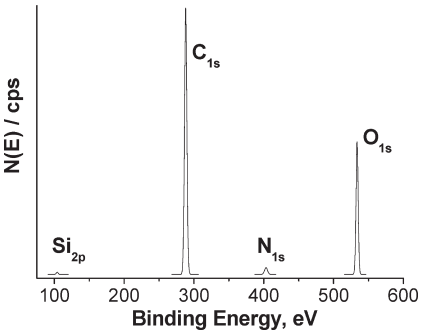

Figure 13. XP Spectrum of the V-npD Sample Showing the Presence of Si and N.

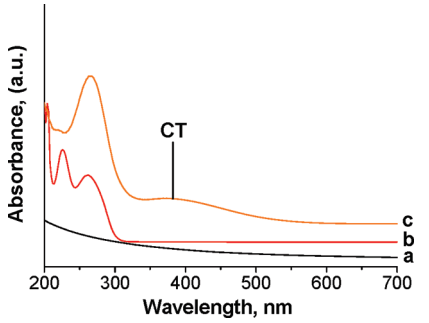

Figure 14. UV−vis spectra of (a) control reaction of (3-chloropropyl)-trimethoxysilane with npD, (b) *N*-methyl-*N*′-(trimethoxysilyl)viologen, and (c) V-npD having I^- as counteranion. CT indicates the position of the charge transfer band between I^- and V (see text below).

absorption band at 280 nm in the UV region in optical spectroscopy and by the intense C=N stretching vibration of the pyridinium rings appearing at 1640 cm^{-1} in FT-IR spectroscopy.

Also the characteristic peaks corresponding to the aliphatic groups and the Si−O bonds could be observed in IR appearing at 3050, 2926, and 830 cm^{-1}, respectively. Comparison of the optical spectra a and c in Figure 14 and the FT-IR spectra c and d in Figure 15 visually demonstrates the different ability of raw npD and HO-npD to undergo functionalization and the superior performance of HO-npD for this purpose.

As commented earlier in this section, attaching covalently viologen units to the diamond nanoparticles renders the resulting sample that should be capable to form charge transfer (CT) complexes. The formation of these CT complexes between covalently attached viologen as

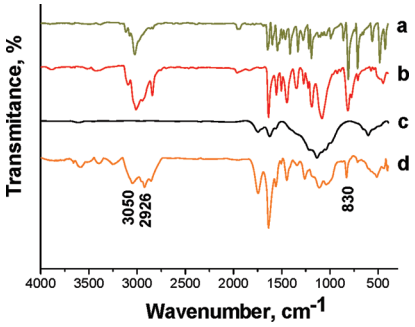

Figure 15. FT-IR spectra of (a) 1-methyl-4-(4′-pyridyl)pyridinium iodide, (b) *N*-methyl-*N*′-(trimethoxysilyl)viologen, (c) control reaction of (3-chloropropyl)trimethoxysilane with pristine npD, and (d) V-npD.

electron acceptor and an electron donor in solution can be visually observed by coloration of the suspension containing V-npD as well as in optical spectroscopy by the appearance of a broad featureless band in the visible region. As can be seen in Figure 14 (spectrum c) upon addition of sodium iodide to an aqueous colloidal suspension of V-npD, the characteristic CT band with λ_{max} 385 nm was recorded. It is well-known that viologens as charge acceptors form strong CT complexes with iodide as charge donor.[69] Thus, covalent attachment of viologen units to npD nanoparticles introduces the property of CT complex formation in this nanoparticle type.

Conclusions

In the present work, we have shown that Fenton treatment has a profound positive influence on the ability of diamond nanoparticles to undergo covalent functionalization. Single-wall carbon nanotubes require purification and activation by HNO_3/H_2SO_4 acids mixtures. Similar treatment fails to produce any effect in pristine npDs due to their higher inertness. In contrast to the HNO_3/H_2SO_4 treatment, Fenton reaction destroys the undesirable soot matter that causes agglomeration of the nanoparticles and makes difficult the preparation of suspensions in which the individual nanoparticles are present. On the other hand, the Fenton treatment increases the population of surface hydroxyl groups that are the reactive sites that can be used for subsequent covalent attachment of a large variety of functional groups. To illustrate the wide range of possibilities, we have here performed reactions that involve C−O bond rupture and replacement by other types of carbon bonds (bromination and arylation) as well as other approaches that are based on the cleavage of the O−H bond and replacement by other O−X bonds (silylation). All together, our work illustrates possibilities opened up by the Fenton treatment for diamond nanoparticles since a parallel study with pristine npD leads only to very poor, in many cases undetectable, functionalization. Considering the present and emerging applications of diamond nanoparticles, an efficient strategy for high-density functionalization will be useful for to develop modified npD nanoparticles with the targeted properties.

Experimental Section

Materials and Instrumentation. All the solids were analyzed by combustion chemical analysis performed in a FISONS CHNOS analyzer. ^1H and ^{13}C NMR spectra for soluble molecules were recorded in CD_3OD or [d_6]-DMSO as solvents on a Bruker 300 MHz apparatus. In the case of the $MeOC_6H_4$-npD sample, the ^1H NMR spectrum was recorded using a Varian Gemini 400 MHz spectrometer. Chemical shifts are given in δ (ppm) using TMS as internal standard. UV/vis spectra were recorded in transmission mode on a Shimadzu UV−vis spectrophotometer. The samples were placed in UV quality quartz cuvettes, 1 cm path length. FT-IR spectra were recorded on a Nicolet 710 FT-IR spectrophotometer using KBr disks or self-supported wafers compressed to 2 Ton × cm^{-2} for 2 min. The size of the nanoparticles was determined by transmission electron microscopy (TEM) using a Philips CM300 FEG system with an operating voltage of 100 kV. TEM samples were prepared by placing microdrops of diamond nanoparticles solution directly onto a copper grid coated with carbon film (200 mesh). Unless otherwise indicated, solvents and reagents were purchased from Aldrich and used as received. Powder XRD were recorded using a Philips X'Pert diffractometer using the KCuα radiation at a scan rate of $2^o \times min^{-1}$.

Fenton Treatment. Raw npD (1 g) commercially available from Aldrich (Diamond nanopowder, 95+%, ref: 636444) was suspended in distilled water (50 mL) in a 500 mL open flask and mixed directly with $FeSO_4.7H_2O$ (5 to 20 g) as source of Fe^{2+}. After complete dissolution of the ferrous salt, concentrated sulphuric acid (10 to 30 mL) was added to the slurry and the corresponding volume of H_2O_2 (30 v/v%) (from 10 to 20 mL) was slowly dropped while observing evolution of CO_2. (***Caution****: H_2O_2 is a strong oxidizer. The Fenton reaction at high concentration is highly exothermic and occurs with evolution of heat and gases. The process has to be done in a well-ventilated fume hood wearing the appropriate personal safety items.*) This slurry was sonicated on an ice-refrigerated ultrasound bath and held at 1−5 °C for 5 h. Within the first 30 min, the solution turned green/yellow colored, indicative of iron oxidation After 1 h, additional amounts of H_2SO_4 and H_2O_2 can be added while the suspension becomes yellowish. This cycle consisting in addition of reagents and sonication can be repeated, allowing the final cycle to occur for longer times to ensure the complete decomposition of H_2O_2. The sample denoted throughout the text as HO-npD was obtained treating raw npD with the highest quantities of $FeSO_4$-$7H_2O$, H_2SO_4, and H_2O_2 and performing two consecutive (reagent addition)−(one hour sonication) cycles. The sample whose FT-IR is shown in Figure 2 (plot b) and denoted as treated with moderate Fenton conditions was obtained with 10 g of $FeSO_4 \cdot 7H_2O$, 15 mL of H_2SO_4, and 15 mL of H_2O_2 and one cycle of reagent addition−one hour sonication.

An analogous Fenton treatment using commercial HiPCO (high pressure carbon monoxide) SWNT (Carbolex, 100 mg) suspended in distilled water (5 mL) using $Fe(SO_4) \cdot 7\ H_2O$ (500 mg) and H_2SO_4 (1 mL) and H_2O_2 (1 mL, 30 w/w %) at 1−5 °C for 1 h leads to complete disappearance of the morphology and properties of SWNT. Thus TEM (Philips CM300 FEG system with an operating voltage of 100 kV using a carbon coated copper grid) shows mostly amorphous carbonaceous particles with almost complete absence of nanotubes. Likewise, Raman spectroscopy (RENISHAW in Via Microscope with 785 nm excitation diode laser and averaging 10 scans of different areas of the black solid) did not exhibit the characteristic radial breathing mode (RBM) band specific of SWNT at about 180−250 cm^{-1}.

In the case of npDs, after the Fenton treatment, the suspensions were diluted with distilled water and allowed to reach room temperature. The excess of acid was removed performing five consecutive centrifugation-dispersion cycles with Milli-Q water. The diamond nanoparticles sediment at the bottom of the centrifuge tube under these conditions. pH value of the supernatant at the fifth centrifugation-dispersion cycle was neutral. Finally, the Fenton-treated npDs were submitted to overnight freeze-drying to obtain a brownish dustlike material. The HO-npD sample obtained using the highest reagent concentrations and under the most drastic conditions was used as the starting material for the following synthesis.

Alkyl Group Functionalization of HO-npD. 100 mg of HO-npD were suspended in a solution of triethylamine (0.72 mL, 5.1 mmol) in dry CH_2Cl_2 (15 mL) at 0 °C under an argon atmosphere. The corresponding acyl chloride (5.1 mmol) was slowly dropped. After 1 h reaction, the mixture was allowed to reach room temperature and then heated at reflux overnight. The excess of triethylamine and acyl chloride were removed performing five consecutive centrifugation-dispersion cycles with CH_2Cl_2. The diamond nanoparticles sediment at the bottom of the centrifuge tube. Finally, they were submitted to five consecutive centrifugation−dispersion cycles with Milli-Q water and overnight freeze-drying to obtain a light brown material.

Bromination of HO-npD. Two-hundred milligrams of HO-npD was suspended in a solution of NBS (3600 mg) in dry CCl_4 (25 mL) under an argon atmosphere. After 48 h at reflux, the mixture was diluted with CH_2Cl_2 and allowed to reach room temperature. The excess NBS was removed by performing three consecutive centrifugation−dispersion cycles with CH_2Cl_2. The resulting Br-npD samples sediment at the bottom of the tube under these conditions. Centrifugation−dispersion was carried out three more times using Milli-Q water as medium. Finally, the resulting suspension was submitted to overnight freeze-drying to obtain a light brown dustlike material.

Arylation of HO-npD. Three-hundred milligrams of HO-npD were mechanically mixed with anhydrous $AlCl_3$ (300 mg) in a mortar. The mixture was then suspended in 10 mL of anisole or *N*,*N*-dimethylaniline, which were used as solvents. The slurry was heated at 120 °C under strong magnetic stirring. After 48 h at this temperature, the mixture was diluted with CH_2Cl_2 and allowed to reach room temperature. The excess of $AlCl_3$ was removed by washing the powder with a sodium hydroxide solution in water (pH 14) to form the soluble AlO_2^- that can be removed by performing five consecutive centrifugation−dispersion cycles with Milli-Q water until the pH value of the filtrate was neutral. Finally, the sample was submitted to overnight freeze-drying to obtain a brownish dustlike material.

Functionalization of HO-npD with Heterocyclic Rings. *Synthesis of 1-Methyl-4-(4′-pyridyl) Pyridinium* (***1***). 1-Methyl-4-(4′-pyridyl)pyridinium (**1**) was synthesized by reacting 4,4′-bipyridine (800 mg, 5.12 mmol) dissolved in dry acetonitrile (10 mL) and a solution of methyl iodide (0.320 mL, 5.12 mmol) in dry acetonitrile (10 mL). The mixture was stirred at room temperature for 8 h until complete disappearance of bipyridine and formation of an orange solid. The solvent was then removed under reduced pressure to give a mixture of mono- and disubstituted bipyridine. The pure monosubstituted compound was obtained by treating the solid with acetonitrile to dissolve compound **1**, filtering the solution from insoluble dimethyl viologen, collecting the solution, and removing the solvent under reduced pressure. Compound **1** was obtained with a yield of 70%. ^{1}H NMR (CD_3OD) δ (ppm): 4.27 (s, 3H, CH_3), 7.79 (dd, J = 1.5 and 4.5 Hz, 2H, ArH), 8.27 (d, J = 6.9 Hz, 2H, ArH), 8.65 (d, J = 6.0 Hz, 2H, ArH), 8.80 (d, J = 6.9 Hz, 2H, ArH). ^{13}C NMR (CD_3OD) δ (ppm): 61.2, 122.2, 125.6, 126.4, 142.4, 145.2, 149.7. IR (KBr): ν (cm^{-1}) = 3026, 1966, 1649, 1547, 1415, 1331, 1222, 1199, 812, 710, 564, 485, 432.

Synthesis of 1-(3-Trimethoxysilylpropyl)-1′-methyl-(4,4′)-bipyridinium (***2***). Compound **1** (200 mg, 0.69 mmol) was dissolved in dry acetonitrile (5 mL) and (3-iodopropyl)trimethoxysilane (0.2 mL, 1 mmol) was added at room temperature. The mixture was stirred at reflux temperature for 48 h. After this time the reaction mixture was cooled at room temperature and a precipitate was formed. The red solid was purified by filtration and washed exhaustively with acetonitrile to remove unreacted (3-iodopropyl)-trimethoxysilane and 1-methyl-4-(4′-pyridyl)pyridinium. Compound **2** was obtained with a yield of 80%.

^{1}H NMR (300 MHz, [D_6]DMSO) δ (ppm): 9.39 (d, J = 6.6 Hz, 2H), 9.29 (d, J = 6.6 Hz, 2H), 8.80 (d, J = 6.9 Hz, 2H), 8.78 (d, J = 6.6 Hz, 2H), 4.67 (t, J = 6.9 Hz, 2H), 4.44 (s, 3H), 3.46 (s, 9H), 2.02 (q, J = 7.8 Hz, 2H), 0.62 (t, J = 8.4 Hz, 2H). ^{13}C NMR (300 MHz, [D_6]DMSO) δ (ppm): 148.16, 148.16, 146.59, 145.73, 126.55, 126.08, 63.05, 50.20, 48.09, 24.71, 5.40. IR (KBr) ν (cm^{-1}): 3012, 2933, 2840, 1966, 1639, 1554, 1438, 1345, 1276, 1190, 1083, 819, 710, 578, 501, 448.

Functionalization of HO-npD with ***2***. Compound **2** (50 mg) was suspended in dry acetonitrile (15 mL), and HO-npD (200 mg) was then added. The mixture was stirred for 20 h at reflux temperature then cooled at room temperature and filtered. The solid was washed with methanol and dichloromethane. V-npDs were dialyzed for 3 days with use of a membrane and a saturated solution of sodium chloride as solvent, in order to remove the excess of the silyl derivative and exchange the iodide counterion present in as-synthesized compound **2** by Cl^-. After extensive dialysis, V-npD was purified by performing five consecutive centrifugation−dispersion cycles with Milli-Q water until the UV−vis of the supernatant was transparent in the UV and no absorption band due to viologen was observed.

Acknowledgment. Financial support by the Spanish ministry of Science is (CTQ2009-11583 and CTQ2007-67805-AR07) is gratefully acknowledged. R.M. also thanks Spanish Ministry of Education for a postgraduate scholarship.

Supporting Information Available: Thermogravimetric profiles of C_n-npD samples (PDF); solubility of C_{15}-npD in dichloromethane (MPEG video). This material is available free of charge via the Internet at http://pubs.acs.org.